

Silhouette sensor using sparse detectors

Application to elephant height estimation

Amitabh Shrivastava

A thesis presented to the Department of Physics
for the degree of
Bachelor of Science(Research)

Under the guidance of

Dr. Vishwesh Guttal
Assistant Professor
Centre for ecological Sciences

Dr. G. R. Jayanth
Assistant Professor
Department of Instrumentation and Applied
Physics



Indian Institute of Science

Bangalore, India

April 20, 2015

Silhouette sensor using sparse detectors

Application to elephant height estimation

Amitabh Shrivastava

Abstract

Electronic perimeter monitoring finds a number of applications in homeland and private security, and human-animal conflict resolution. This thesis presents the design and development of a passive ranging and profiling sensor. The sensor system presented detects the location of the object in between the sensing units and a silhouette of the object as it passes between the sensor. The sensor is demonstrated to have a < 1 inch resolution in measuring height. Since the sensor uses modulated infrared light and is digital, it is practically immune to noise from natural sources. This allows for the sensor to have a long range of > 20 m without any focusing lenses. The range can be extended to hundreds of meters with single lens optics. Cellphone communication is incorporated to transfer the data wirelessly. Local data storage allows the sensor to be used in areas without cellphone connectivity. The sensor also acts as a camera trigger and is easily connected to a camera trap. Temperature and humidity sensors are added to collect data on these environmental parameters. Low power consumption design and solar panels allow the sensor to operate completely off the grid. The sensor design is highly modular for easy maintenance and replacement. The modular nature also allows for a range of possible sensor sizes. Weather proofing is done to ensure that the sensor is well suited for field use. The possibility of using the sensor as height measuring tool for elephants is discussed.

Contents

1	Introduction	3
2	Motivating Application	4
3	Description of the technique	7
4	Implementation: Electronics and Design	12
4.1	Control	12
4.2	Detectors	12
4.3	Infrared LED's	13
4.4	Arrays	14
4.5	Power management	14
4.6	Peripherals	15
4.7	Weather Proofing	16
5	Experimental validation	16
5.1	Detecting height	17
5.2	Detecting Distance	17
5.3	Silhouette detection	18
5.4	Partial 3D reconstruction	19
6	Discussion	20
7	Conclusions	21
8	Acknowledgments	21

1 Introduction

Electronic perimeter monitoring finds a number of applications in homeland and private security, and human-animal conflict resolution. Monitoring of political and private boundaries against intruders is of obvious significance. Settlements in human-animal conflict zones need to monitor their boundaries against animal intrusion for safety. Roads and railways need to monitor ecological perimeters to prevent accidents.

It is desirable for a perimeter monitoring system to produce as few false alarms as possible while maintaining a high detection rate. For this, it is important to collect enough information about an intrusion to allow threat type categorization. Any field deployable monitoring system should also be immune to noise from natural sources. For monitoring long perimeters in the field, it is also important for the system to be power efficient and robust against the elements. Relatively few of the conventional sensing technologies satisfy these criterion.

Simplistic systems such as tripwires while very power efficient and robust; provide little information about the type of intrusion. And complicated systems such as video surveillance collect so much information that automated detection is nearly impossible. One way to collect relevant information about an intrusion is to detect the silhouette of the intruder. This allows for possible categorization of a large range of possible threat types. Since each pixel in the image of a silhouette is binary, image processing is much easier as compared to images from a video.

A silhouette detector can be used to extract linear size parameters such as height of an object passing through it. To do this effectively, the detector needs to be of very high resolution. For example: to detect heights of elephants accurately, it is desirable for the detector to have a resolution ~ 1 inch.

Optical beam interruption is a simple sensing technology based on the blocking of light path between an optical emitter and detector. It has been well used in perimeter monitoring due to its simple operating principle, ease of setup and passive nature. This technology has been used before as a silhouette/height profile detector in at least two different ways:

- Using analog receivers[1]

In this method two light emitters (operating at different frequencies) with adjacent analog receivers are placed at different heights on one side of a trail to be monitored. Directly opposite to the emitters is a retro-reflective strip. In the absence of an object blocking the path, the whole retro-reflective strip is illuminated by the emitters and therefore light intensity at the receiver is the highest possible. If an object blocks the light path, the shadow it casts on the retroreflector reduces the

reflective area and by knowing the reduction in light intensity at the two receivers, the distance of the object to the sensor and blocking height can be known.

- Using multiple digital receivers [5]

In this method, multiple light emitters with a narrow field of view and adjacent digital receivers are stacked one on top of the other on one side of a trail. On the other side, multiple small pieces of retro-reflective tape are placed opposite to each emitter/receiver. When unblocked by an object, each of the receivers observes a high light intensity however, when blocked, the receivers not receiving the light form a silhouette of the object directly.

The analog sensor technique provides the amount of blockage offered by the object instead of a silhouette. While this is sufficient for objects close to the ground, e.g. most vehicles; the method fails for animals like elephants with a large clear area under the belly. The multiple digital receiver approach suffers from a very short range and is prone to misalignment because of the narrow field of view. It also fails to provide the distance of the object to the sensor. Also, neither of the methods can provide sufficient resolution for height measurement of an object passing through the sensor.

Here I propose a high resolution optical beam interruption based silhouette detection and ranging sensor. The sensor combines features from both of the techniques proposed above. It provides a true silhouette of the object but is able to simultaneously measure the distance to the object. The emitters have a large field of view like in the case of the analog sensors and are thus immune to misalignment. Since the receivers are digital, they are immune against miscalibration due to e.g. dirt on the sensor. It utilizes a vertical array of infrared emitters and detectors placed opposite to each other across a trail to be monitored. By eliminating the retroreflector, the effective light path is halved thus giving a much larger range.

2 Motivating Application

Demographic data of wild populations of animals is important for understanding their ecology and behaviour. One of the most important demographic data for modeling population dynamics is the relative proportion of individuals in different age-classes in a population (age structure). For example, knowing the reproductive population of a specie is important for estimating future populations. Such information is especially relevant for endangered species such as the Asian elephant. Poaching and human-animal conflict are the major threats to the Asian elephant in India. These threats are directed mainly towards adult males and therefore can skew the population structure. Effective conservation measures should take this into account, and thus demographic information is a valuable tool for conservation.

Although the proposed technique of silhouette detection is more widely applicable, it was motivated out of the need for a high resolution height measuring device for elephants. Elephants grow throughout their lives, their height can be used as surrogate for age[6]. The sensor can therefore be used to obtain elephant demography information. Currently, elephant height information is obtained mainly via photographic methods. There are several variations on the technique which can be categorized into two classes:

- Using a scale object

The technique relies on photographing the animal and having an object of known size at the same position. This can be obtained by photographing the animal and later placing a scale object such as a pole at the same position as the animal and photographing from the same location, as described in [3]. Or by projecting parallel laser lights on the animal with known separation between them, as described in [4]. Either way, the height of the animal is calculated as

$$H_a = \frac{H_s * N_a}{N_s} \quad (1)$$

where H_a = Height of the animal, H_s = Size of the scale object, N_a = Number of pixels occupied by height of animal, N_s = Number of pixel occupied by scale object

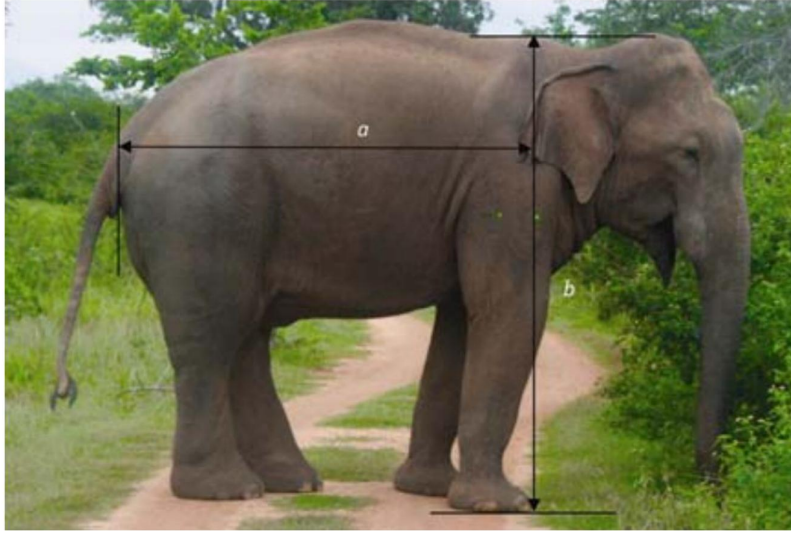


Figure 1: Image source [4]

Photograph of an elephant with two green laser points on the right leg placed 20cm apart as scale object. The height is calculated using equation 1. Note that the top of the shoulder and end of the front foot are used as reference points for measuring height.

The method poses challenges as the undulations on the ground limit the accuracy of measurement [2]. The pole technique especially is time consuming as one has to wait for the animal to pass and get another photograph to complete the measurement.

Also, one cannot be sure where the animal stood exactly, especially in grassy terrain. The laser technique poses challenges as well as. The uneven nature of the animal can potentially reduce the accuracy of measurement and the laser can possibly harm the eyes of the animal.

- Using distance and camera optics

This method involves knowing the distance to the imaged object and the focal length and magnification of the camera lens used [3]. The height is calculated as

$$H_a = \frac{D_a * H_i}{F} \quad (2)$$

where H_a = Height of the animal, D_a = Distance from the camera lens to the animal, H_i = The height of the image (Number of pixels occupied * Size of the sensor/Pixels per meter of the sensor), and F = Focal length of the camera lens.

The method suffers from many shortcomings not the least being the fact that accurate distance measurement to the position of the animal can be very time consuming (with a tape measure or similar instrument) or unreliable in sunlight and limited in range (using a laser rangefinder).

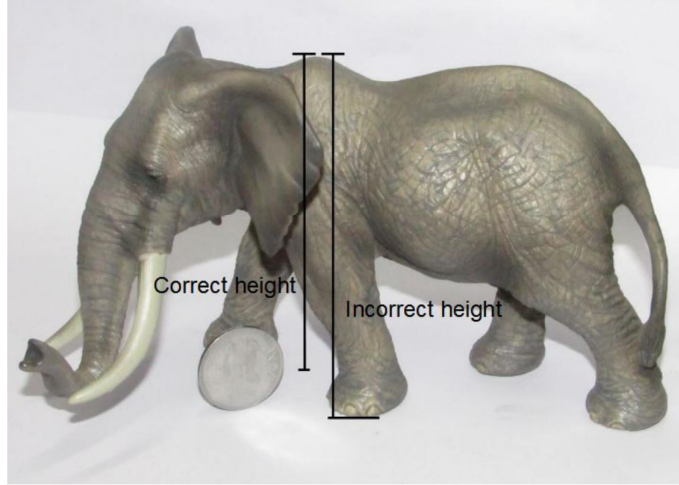


Figure 2: A toy elephant with a coin for scale to show the effect of projection on height measurement. The correct and incorrect heights are marked. The incorrect method of measuring height overestimates the height by $\sim 15\%$.

The photographic technique is essentially extracting 2 dimensional information from 3 dimensional objects. It therefore suffers from projection effects. Consider the image shown in figure 2. To get the height at shoulder, one needs to measure the number of pixels occupied by the height. Since there is a scale object (a coin) in the image itself, the height can then be easily calculated by (1). To get the correct vertical height, the number of pixels between the top of the shoulder and the point on the ground vertically below

should be considered. But, it is unclear which pixel corresponds to such point. Often the bottom of the foot facing the camera is taken as the second point[Fig. 1]. If one were to use this in the figure 2 the height would be overestimated by $\sim 15\%$. Admittedly, this projection effect becomes less and less important as the distance to the animal increases. Nevertheless it is of significance as other sources of error(e.g. reduced resolution due to lower number of pixels occupied in a fixed focus camera) increase as the distance increases. Hence the photographic method does not work very well for any distance to the target animal.

3 Description of the technique

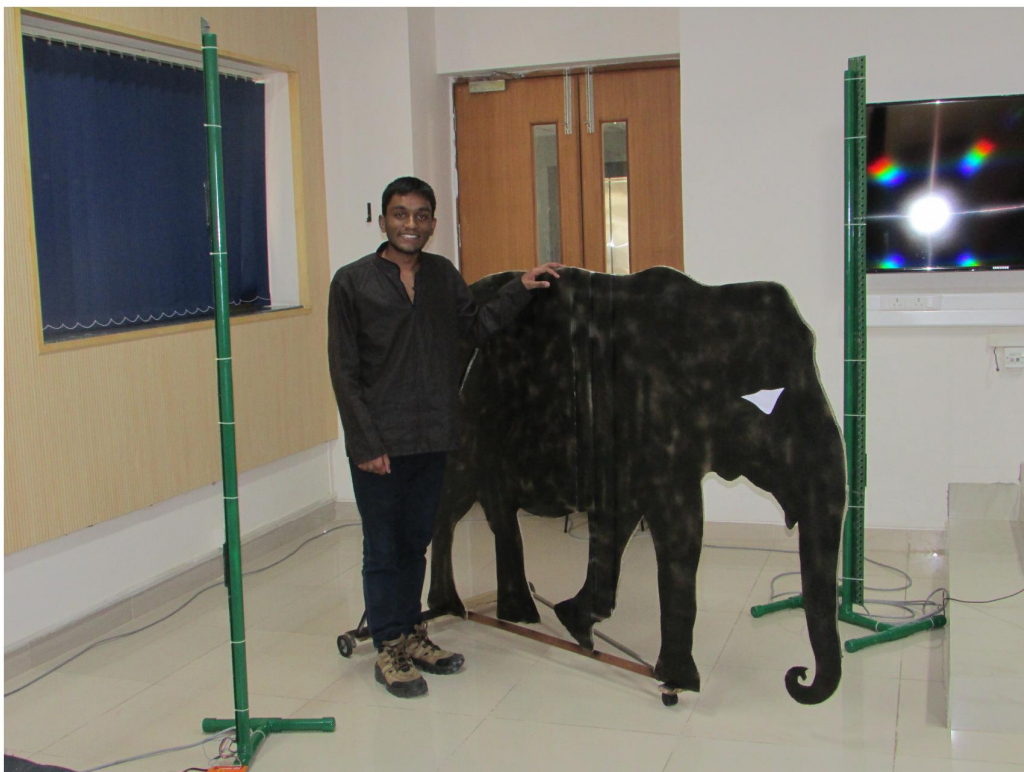


Figure 3: A photograph showing the bare emitter(left) and detector(right) circuit board arrays without the weatherproof casing. An elephant cutout and a human are blocking the light path.

Note: This small(6'6") array was used for all the experiments described in this report. This unit was fabricated as it can be easily implemented in a lab setting. A larger 13' board was also fabricated for field deployment; but was not used due to its prohibitively large size.

Fig. 4 shows a simplified cartoon of the sensor with the emitter and detector array placed across the trail to be monitored. While only four emitters and detectors are shown for simplicity, the prototype constructed uses 156 emitters and detectors. The emitters

$(E_1 - E_4)$ are divergent light sources such that the light from any of the emitters is detected by all of the detectors $(D_1 - D_4)$. The figure also shows the possible light paths when an obstruction of height h is present at a distance x from the emitter array. The unobstructed light paths are shown in solid lines, while the obstructed paths are shown as dotted lines.

The simplest way to measure height using the apparatus would be to switch on the emitters one by one and to check if the corresponding detector detects the light. The highest detector to not receive the light when corresponding emitter is switched on (D_2 in this case) would be at a height less than that of the object. And the detector above it (D_3 in this case), at a height greater than that of the object. Thus the height of the object is found to be between D_2 and D_3 . This method is hereby referred to as the silhouette method of finding height. Note that since the emitter and the detector are at the same height, there is no parallax error. The silhouette method of calculating height however, heavily under-utilizes the sensor and limits the resolution to the inter-detector spacing. A better technique is described below.

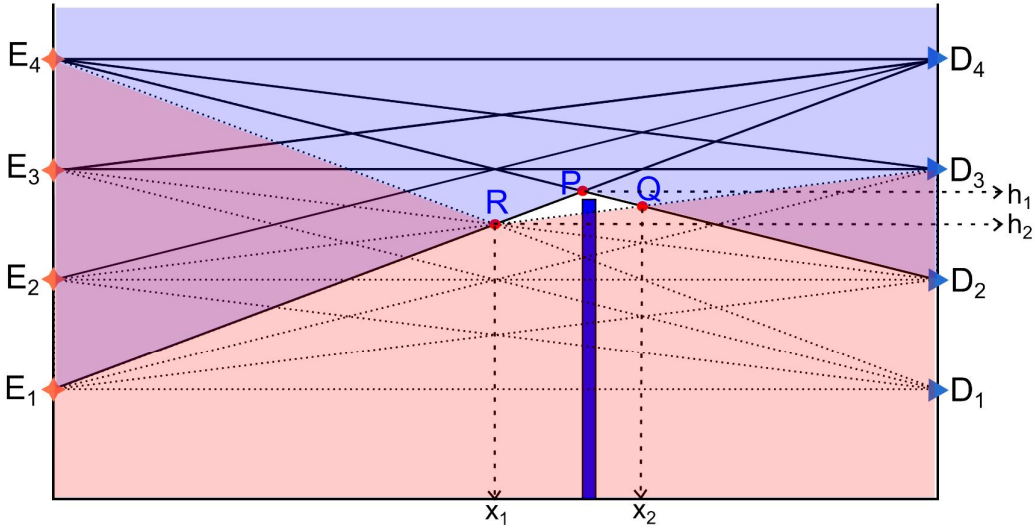


Figure 4: A simplified cartoon showing four emitters(E_1 - E_4) and detectors(D_1 - D_4) with an object(solid blue) blocking the light path. Unblocked light paths are shown as solid lines, blocked light paths are shown as dotted lines. Since all the light paths in the blue region are unblocked, the object cannot be in this region. Since all the light paths in the red region are blocked, top of the object must lie outside this region. Therefore the top of the object is located to within the PQR white triangle. The height of the object is thus known to be between h_1 and h_2 and distance to between x_1 and x_2 .

In Fig. 4, since all of the light paths contained completely in the $E_1PD_2D_4E_4$ (blue) region are unobstructed, the top of the object must lie below this region. Similarly, since all of the light paths contained completely within the $E_4RD_3D_1E_1$ (red) region are obstructed, the top of the object must lie above this region. Thus the top of the object is located to within the PQR (white) triangle. The height and location of the top of the

object are then known to be within $[h_1, h_2]$ and $[x_1, x_2]$ respectively. This method gives a better resolution of the height of the object and also provides an additional parameter viz. the distance of the object in between the emitter and detector. While not of much value by itself, the distance to the object can be an important parameter if the sensor is paired with a camera trap, in which case other measurements of the object can be obtained by using the photographic technique.

Note that while the location of the top of the object is known, the form of the object below the top is still unknown. The situation becomes much more complicated in the case of an object with holes or a floating cross-sections; for example the belly of an animal crossing the sensor. But, similar analysis can reveal the location of the top and bottom of the object. In case of objects with structure along the emitter-detector axis similar analysis can reveal details about the 3D structure of the object. In the figure 5 the light path is blocked by an extended object. Since all the light paths contained in the blue region are unblocked, the object must lie below this region. Note that the form of the bottom of this region roughly follows the shape of the object itself. But, to make strong predictions on the size of the object, assumptions about the shape need to be made.

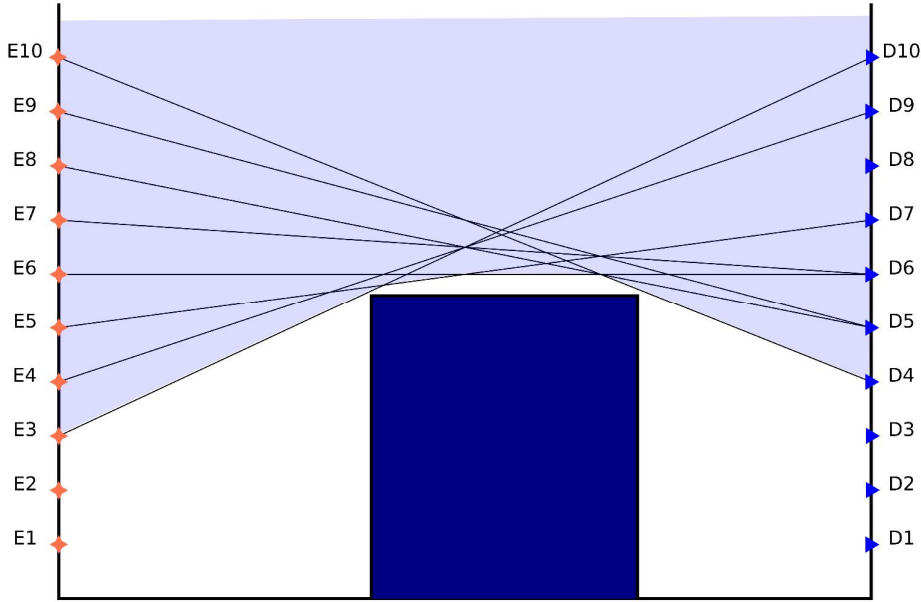
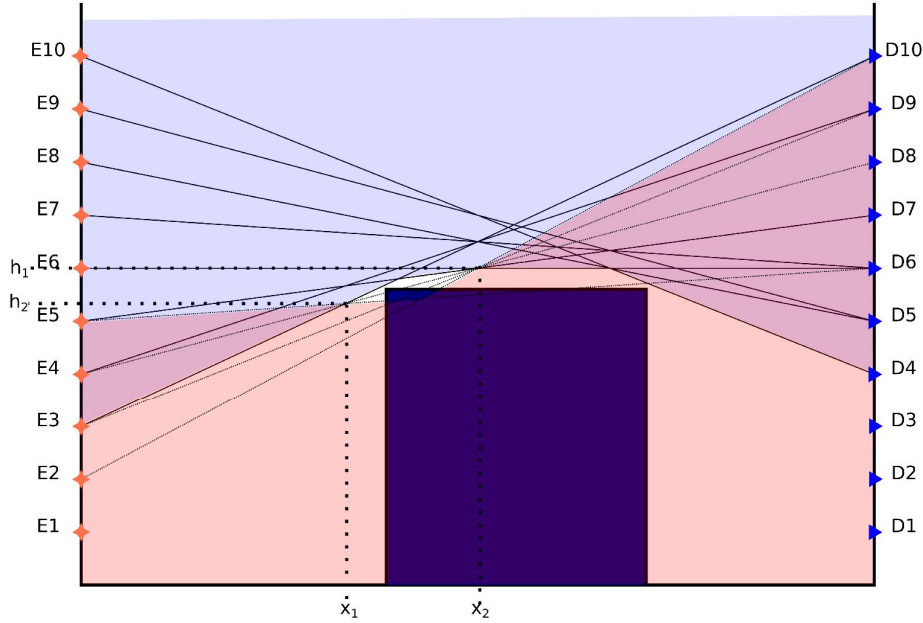
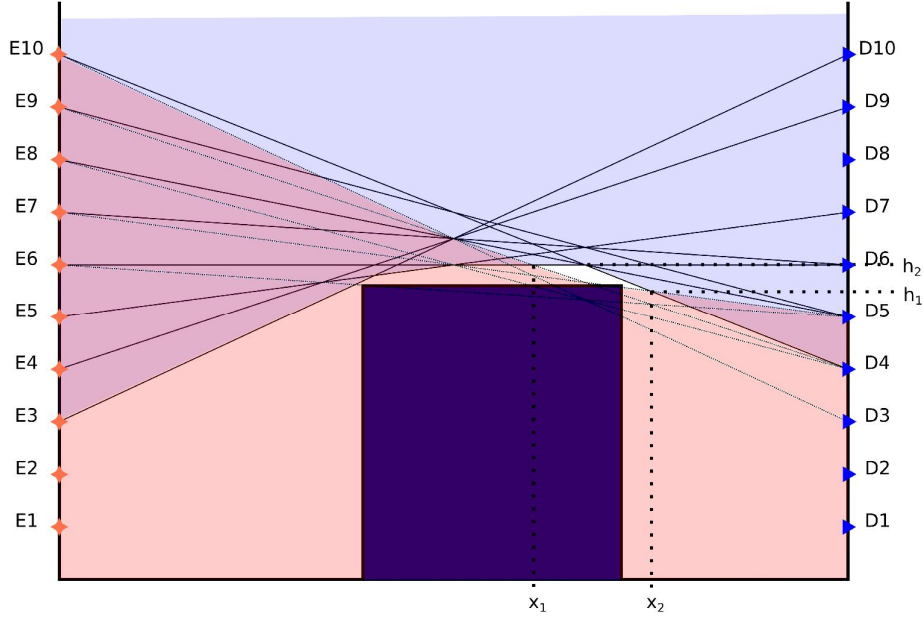


Figure 5: A simplified cartoon showing ten emitters and detectors with an extended object blocking the light path. The since all light paths contained completely in the blue region are unblocked, the object must be in the white region.

Assuming a rectangular geometry of the object, the problem of finding width of the object can be broken down into two. By considering the emitters below and above the height of the object(found through the silhouette method) the position of the corners towards and away from the emitter array can be found.



(a) The corner of the object towards the emitter located to within the white quadrangle using data from emitters below the height of the object.



(b) The corner of the object towards the emitter located to within the white quadrangle using data from emitters above the height of the object

Figure 6: A cartoon describing how information about width can be extracted from the sensor. Unblocked light paths are shown as solid lines, blocked light paths are shown as dotted lines. Since all the light paths in the blue region are unblocked, the object cannot be in this region. Since all the light paths in the red region are blocked, top of the object must lie outside this region. Therefore a corner of the object is located to within the white region.

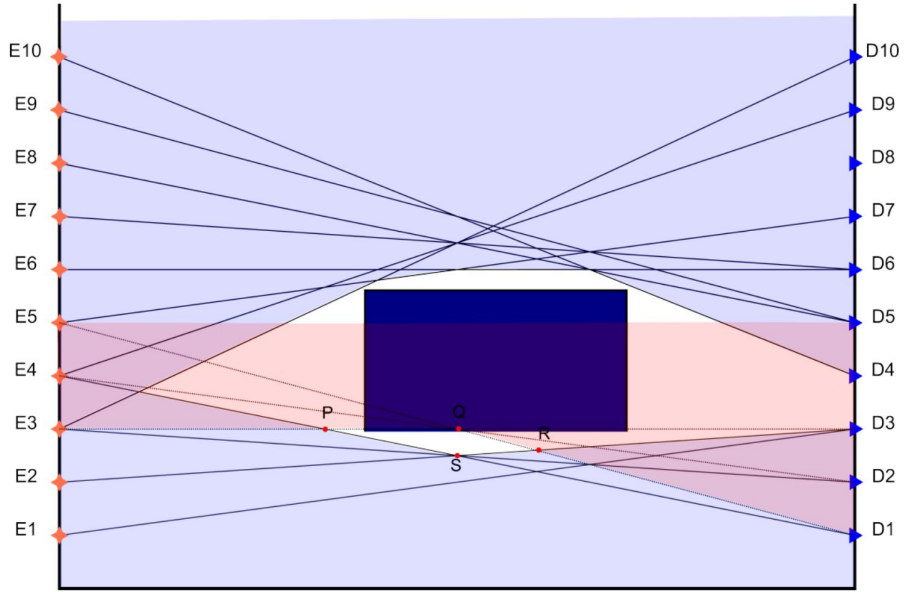


Figure 7: A simplified cartoon showing ten emitters and detectors with a floating object(solid blue) blocking the light path. Such a scenario can exist when an animal passes through the sensor and the belly of the animal is being detected. The location of the bottom left corner of the object is located to within the white quadrangle $PQRS$ using the blocked light paths from emitters above the bottom of the object and traveling downward. The location of the other corners can be found similarly.

4 Implementation: Electronics and Design

The sensor was designed to be a field deployable data collection unit. Fig. 8 shows the basic block diagram of the sensor.

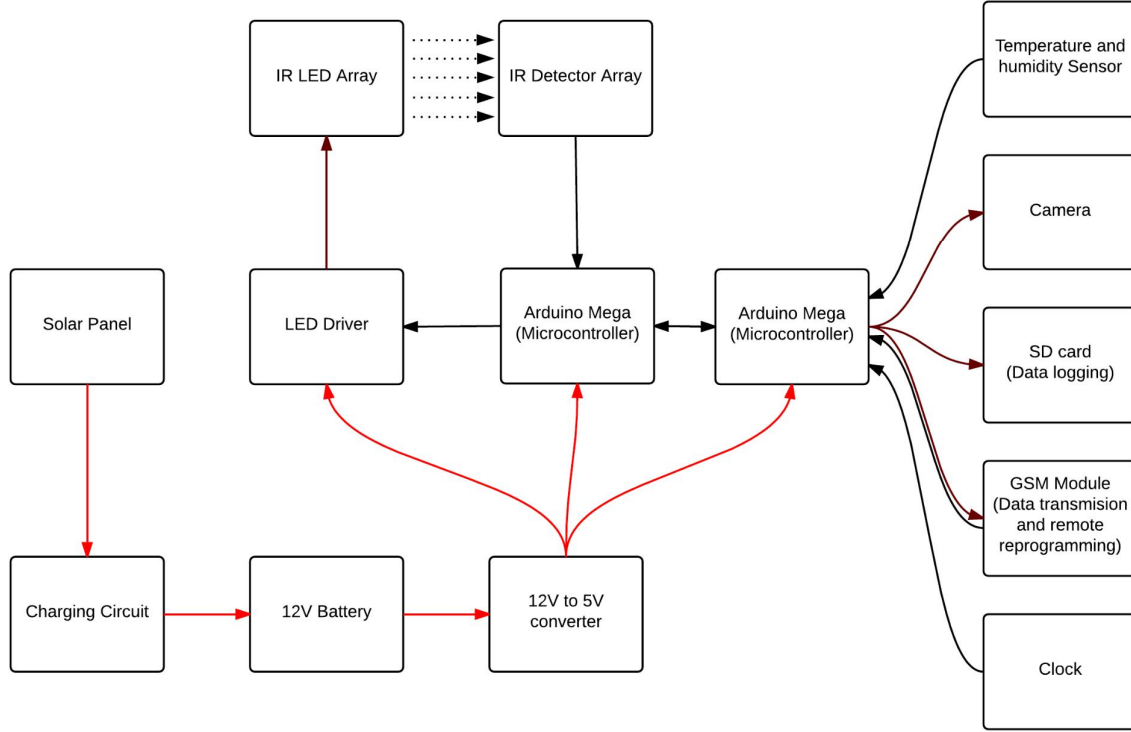


Figure 8: Block diagram of the design of the electronics involved in the sensor. Red arrows represent the flow of power, black arrows represent the flow of data and brown arrows represent the flow of both data and power.

4.1 Control

At the heart of the unit are two ATmega2560 micro-controllers in the form of Arduino Mega responsible for (a) communicating with and controlling the emitter and detector arrays and (b) communicating with and controlling data storage, camera trap and other peripherals. The Arduino platform was chosen for its ease of use, easy availability and proven robustness. Communication with the emitter and detector arrays takes place over the same high speed (400KHz) I2C bus which keeps wiring connections to a minimum.

4.2 Detectors

The *TSSP4038* sensors used are similar to those used in most infrared remote control systems. Their wide use serves as an advantage as they are well tested and cheap due to mass production. The sensors were also chosen for their ease of use. They are available

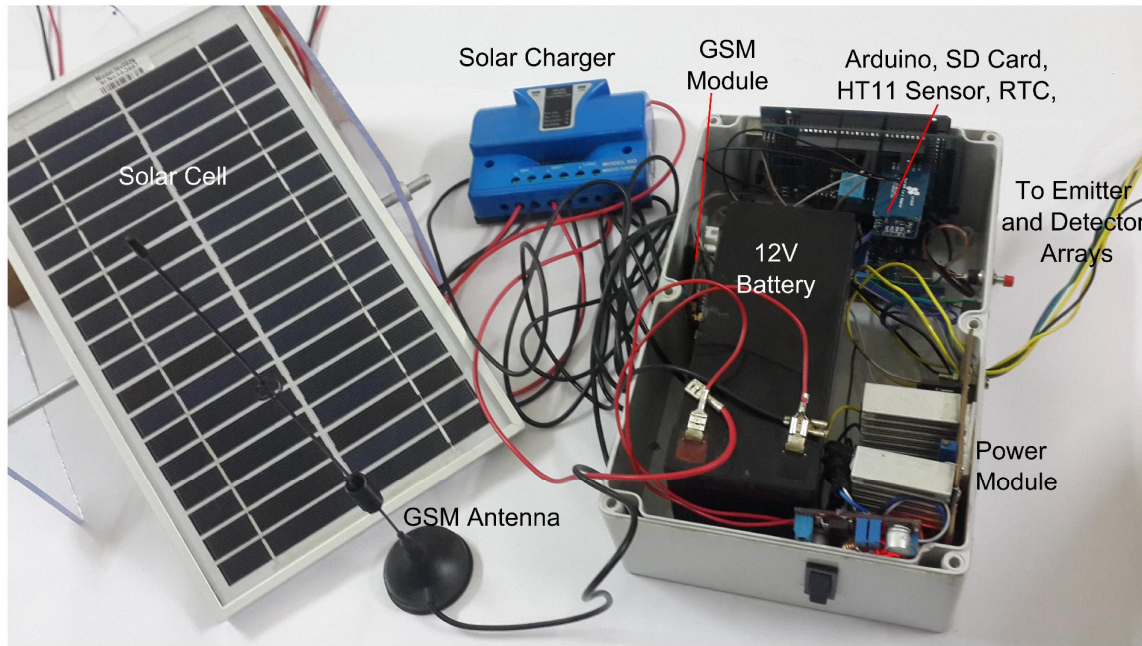


Figure 9: A photograph of the electronics in a weatherproof box. The individual components are marked. All circuits except the power module are bought off the shelf and are used with little modification.

in a 3 pin DIP form factor with a digital output indicating the presence or absence of pulsed IR light. Specifically, the sensors are selectively responsive to $950nm \pm 80nm$ light pulsed at $38KHz$. This is ensured by an IR selective filter encasing the sensor and a band pass filter tuned to $38KHz$ built into the sensor. Since there are no natural sources of $38KHz$ pulsed light and because of the inbuilt amplifier, the sensors can respond to extremely low intensity of light ($\sim 0.4mW/m^2$). The sensors have a broad field of view of $\sim 60^\circ$ FWHM which gives a lot of room for misalignment between the emitter and detector arrays without affecting performance.

4.3 Infrared LED's

The TSAL6100 LED's were chosen for their high intensity and field of view of 20° FWHM which allows for some misalignment while maintaining high range. The LED's emit light at a narrow band ($30nm$ FWHM) around $940nm$ peak wavelength which matches well with the detector acceptance band around $950nm \pm 80nm$. Two LED's are connected in series for each emitter such that the intensity at the receiver is doubled. Thus increases the maximum distance between the emitter and receiver arrays while increasing the power consumption only nominally.

The LED's are driven using a low side darlington switch (ULN2803) and a high side switched constant current driver (figure 11).

4.4 Arrays

The infrared LED/detector array consists of 156 elements placed 1 inch apart each for a total array length of 13 feet -the height of the tallest African elephants. Custom printed circuit boards are designed and fabricated to give full control over the placement of the emitters/detectors. An array consists of four circuit boards connected in series. Each circuit board is 3'3" in size. Since most circuit board manufacturers do not produce boards of this size, each circuit board is broken down into two sections which are soldered joined later. To keep the cost of prototyping low, the circuit board is designed such that the same board can be used as a detector/emitter array by simply changing the components mounted on the board.

Given the large number of elements which need to be individually controlled, it is prohibitive to dedicate a separate pin in the micro-controller to each emitter/detector. Hence a PCA9505 multiplexer/demultiplexer is used to connect the elements to the micro-controller. Each PCA9505 has 40 I/O pins which can be accessed by the micro-controller via I2C communication. The PCA9505 has a three bit address which allows for 8 of these to be connected to the same I2C bus. Thus the micro-controller can access $8*40=320$ I/O pins.

Each array consists of four sets of 39 elements connected to 39 pins of a PCA9505. One pin is purposely left unused for future expansion using additional sensors e.g. incorporating temperature sensors for automatic shutdown in case of overheating. In this way, $39*4=156$ LED's and sensors are connected to the micro-controller. Since the detector is then made up of four identical PCBs stacked together, repairs also become easier. The PCBs for the array are designed to accommodate both the LED's with the low side switches and the detectors with simple jumper connection changes and different placement of components.

NOTE: All of the experiments described in this report are performed using a smaller 78 element(6'6") array which is easier to implement in a lab setting.

4.5 Power management

The unit is powered via a 12V lead acid battery; chosen for their wide availability, robustness and long life. The incorporation of a solar panel and charger allow for the unit to run autonomously, off the grid for months at a time. An off the shelf switch mode power supply module is used to convert the 12V into a more readily usable 5V. The total power consumption by the unit is $\sim 2W$. The power consumption can be brought down further by using custom circuit boards instead of the Arduino boards.

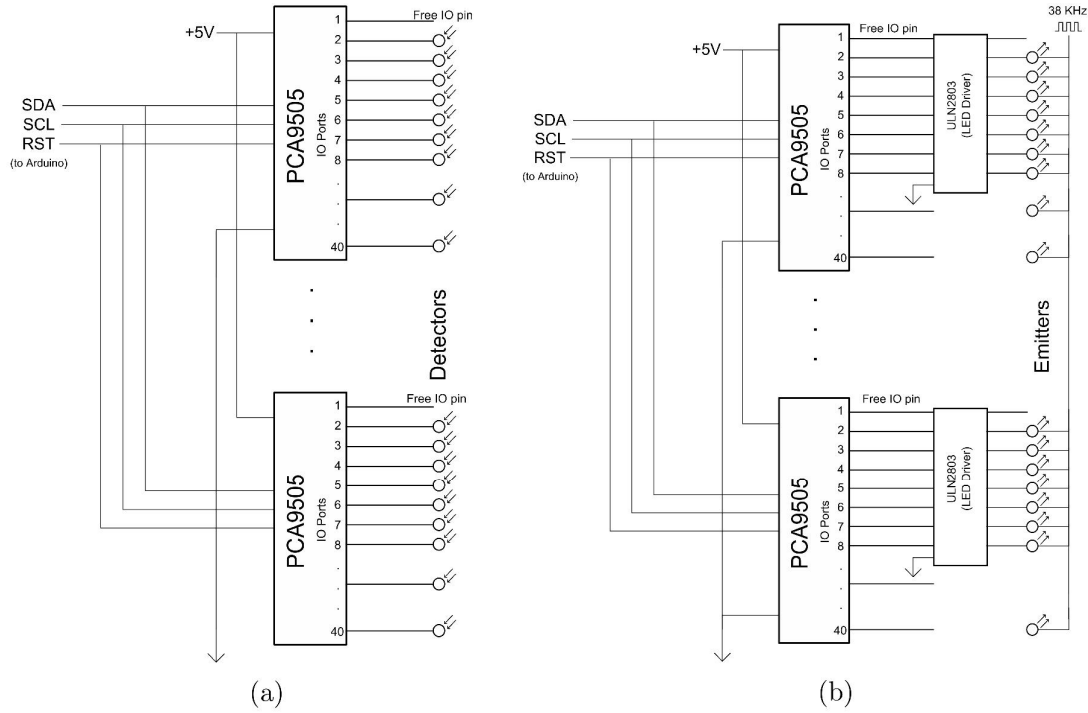


Figure 10: A simplified circuit diagram of the detector and emitter arrays. Four PCA9505's are to be used in the field deployable sensor. Communication to Arduino happens via 400KHz I2C over SDA and SCL lines. The reset pin of PCA9505 is broken out to the Arduino as well. (a) The detectors are connected PCA9505 mux/demux used as multiplexer. (b) The emitters are connected to the PCA9505's through ULN2803 used as low side drivers. 38KHz pulsed current regulated supply is provided at the high side of the LED's.

4.6 Peripherals

The sensor is meant to be field deployable. Therefore it needs data-logging capabilities. They are provided by a real time clock(DS1307) and an SD card data-logger. Both of the units are readily available and easy to interface with the arduino. Data of each obstruction event is stored along with a time stamp.

To confirm the type of animal passing through the sensor as well as to obtain further information pertaining to gender, identity etc, the sensor is paired with a camera trap. The camera is triggered on the event of an obstruction.

Since the setup allows for easy interfacing of external sensors and has data-logging capabilities, a temperature and humidity sensor(DHT11) is added to the system. Data from this sensor is recorded periodically into the SD card.

To allow for the proposed sensor to be used as an early warning system, a GSM module is interfaced as well. Partial data of the silhouette is sent in the form of an SMS in case

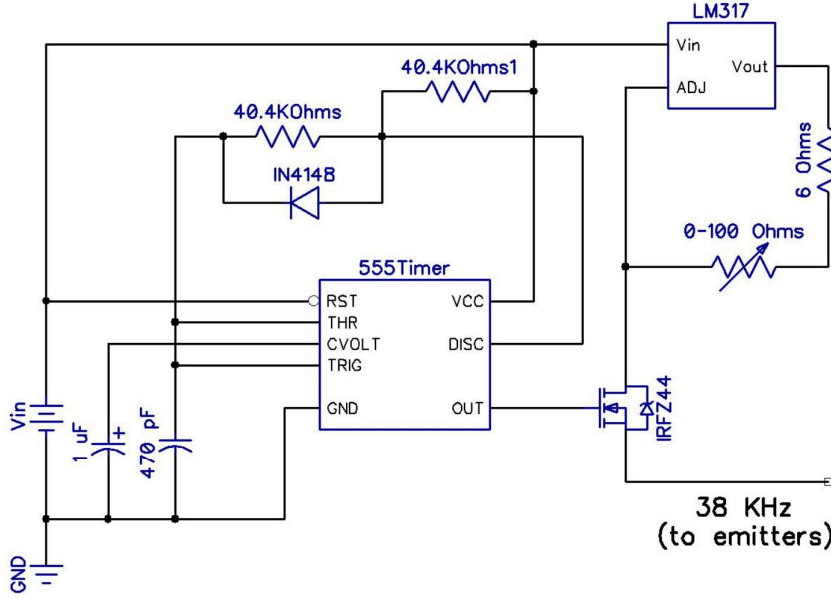


Figure 11: Schematic of the circuit powering the LED's. The circuit is designed to provide 38KHz pulsed constant current of 10-200 mA (varied using the potentiometer). The circuit accepts input voltages ranging from 5V to 35V.

of an obstruction.

4.7 Weather Proofing

The sensor is weather proofed for field use. The circuit board is coated with two coats of acrylic based conformal coating(DC Acryform). This waterproofs the electronics and prevents corrosion. The emitter and detector arrays are then enclosed in a waterproof plywood case with an acrylic front panel for the light pass through. All joints and wire ports are sealed with silicone for water and dust proofing. The outside of the case is coated in two layers of waterproof paint for further protection. The control, power and peripheral circuits are enclosed in an IP65 rated plastic enclosure.

5 Experimental validation

Experiments were done in an open place with paved concrete floor to reduce reflections and to simulate field conditions. Due to the undulations on the surface, all heights are taken with an uncertainty of $\pm 1cm$. The detector and emitter are placed 10m apart for all experiments.

5.1 Detecting height

The heights are calculated by the algorithm mentioned before by placing a cardboard sheet of given height midway between the emitter and the detector. The calculated heights and real heights are plotted in figure12. To take into account the manufacturing tolerances and the physical size of the emitter and detector, an uncertainty of $\pm 1cm$ is taken for all calculated heights. The error in all cases is well within the margin; the maximum error being $1.4cm$. To ensure that the position of the object does not affect the height, the same object was placed at five distances from the sensor. The maximum difference in the measured heights was found to be $1.2cm$; well within the error margin.

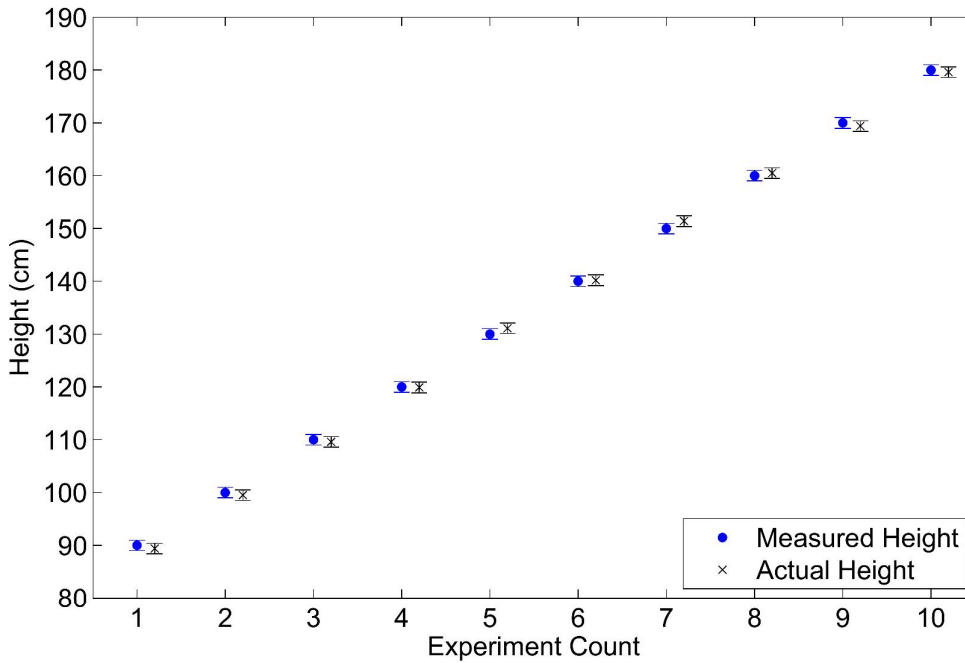


Figure 12: Measured and actual data when objects of various heights were placed $5m$ from the emitter. The maximum difference in measured and actual height was found to be $1.4cm$.

5.2 Detecting Distance

Objects of height $82cm$ and $117.5cm$ were placed at 7 different distances in between the arrays. The distance was calculated using the algorithm mentioned before. The uncertainty in distance depends on the position and height of the object. The maximum difference in the measured distance to the actual distance was found to be $6cm$. Note that the distance resolution varies highly based on the position and height of the object as previously described in the algorithm for measuring distance.

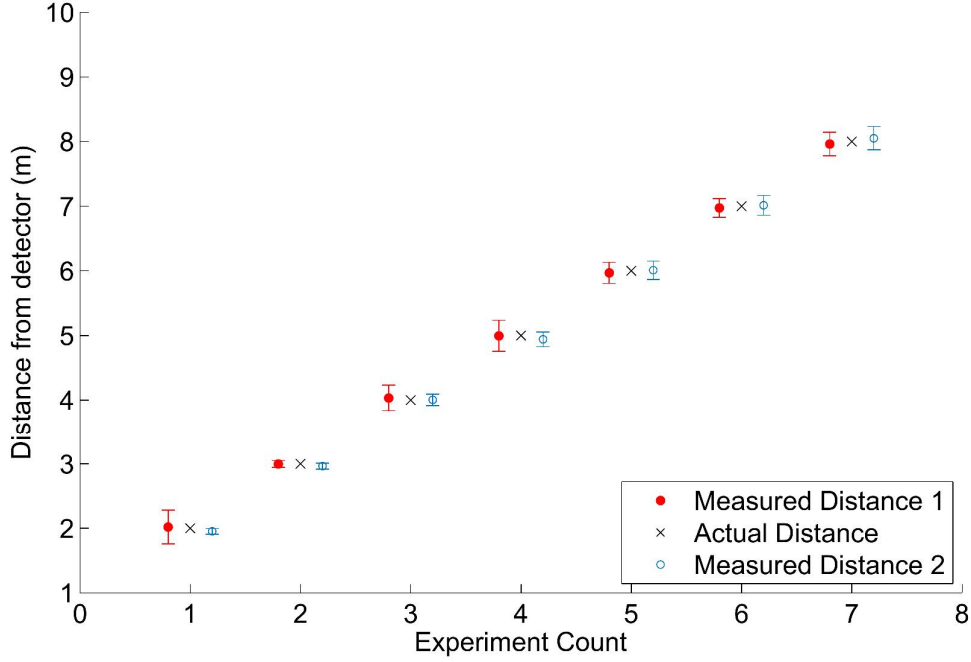


Figure 13: Measured and actual distances when objects of height $82cm$ (red) and $117.5cm$ (blue) are kept at various distances from the detector. The maximum difference in measured and actual distances was found to be $6cm$.

5.3 Silhouette detection

As an object passes through the sensor, it effectively scans itself. And thus a side-view silhouette of the object is obtained [Fig.14].

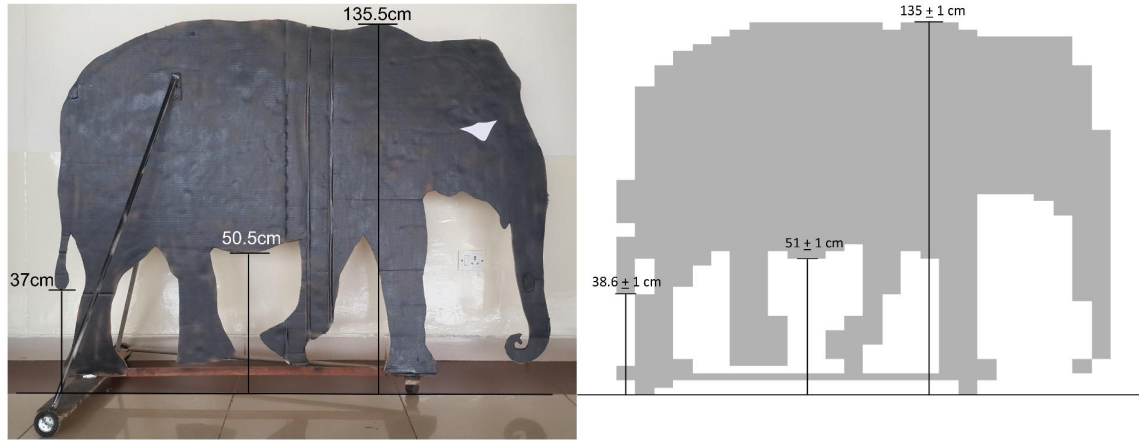


Figure 14: The photograph and silhouette of a cardboard cutout of an elephant are shown. The silhouette is obtained by moving the cutout slowly through the sensor. Heights of some features are marked. The maximum difference in measured and actual height is found to be $1.6cm$.

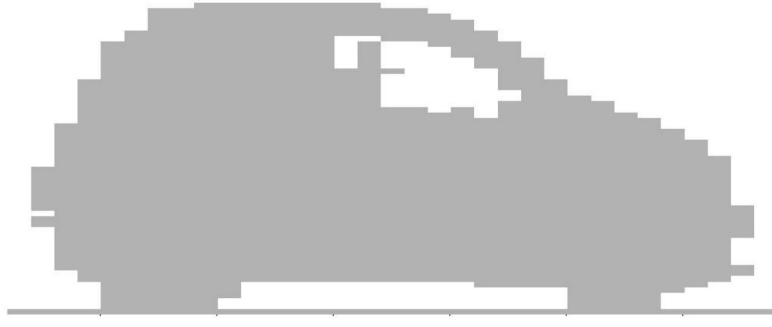


Figure 15: The silhouette of a car obtained by driving the car slowly through the sensor. Note that the rear windows are closed and appear opaque as most of the infrared light is reflected off or absorbed.

5.4 Partial 3D reconstruction

A cardboard box 113.5cm in length and 114cm in height was placed lengthwise in between the sensor. The positions of the corners were calculated by the algorithm mentioned before[Fig. 16]. The maximum difference in the measured and actual height was found to be 1.6cm . The difference between measured and actual length of the box was found to be 2cm .

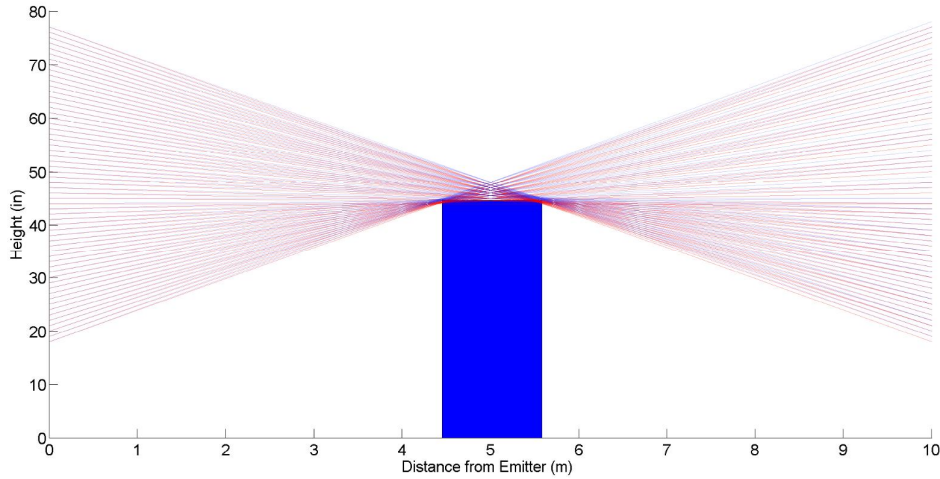


Figure 16: A cardboard box 113.5cm in length and 114cm high was placed 4.45m from the emitter(solid blue). The figure shows the unblocked(blue) and blocked(red) light paths. The maximum difference in measured and actual height was found to be 1.8cm and difference in measured and actual length of the box was found to be 2.5cm .

A plastic table was placed widthwise between the sensor such that only the top of the table blocked the sensor. This creates a floating cross section blocking the light path. Analysis was carried out as mentioned before. The maximum difference in measured and actual height was found to be 2cm . The difference in measured and actual width was found to be 3.5cm .

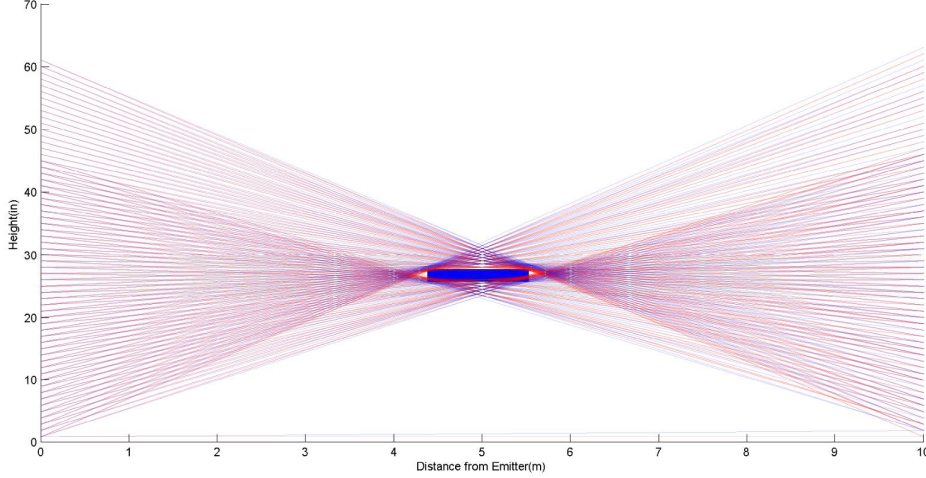


Figure 17: A top of a plastic table covering $67cm$ to $72cm$ in height and $114cm$ wide blocks the light path. The figure shows the unblocked(blue) and blocked(red) light paths. The maximum difference in measured and actual height was found to be $2.1cm$ and difference in measured and actual width of the table was found to be $4cm$.

6 Discussion

The major problem with the detector is the low sampling rate. Because of the long response time of the detectors used and because of the serial mode of sampling, the whole array is only sampled at $2Hz$. This limits the use of the sensor to slow moving, long objects such as elephants. The sampling rate can however be increased by using IR detectors tuned to higher frequency than $38KHz$ and by optimizing the code.

Another drawback of the sensor is the implementation of wired connection between the emitter and the detector arrays. While this allows for a single power supply to power both the units, it can pose to be a major hindrance for installation in the field. This however can be solved by providing separate power sources and using I2C over the air communication between the two arrays.

The sensor was designed for monitoring narrow choke points where elephants are forced into moving in a straight file and there is little overlap between consecutive silhouettes detected by the sensor. Therefore, range beyond $\sim 20m$ was not necessary. However, the range can be extended using converging lens to focus the emitted light and to increase the collecting area of the detector. Preliminary experiments with lenses of 1 inch aperture increased range to well over $100m$. Thus, the system can potentially be used to monitor long perimeters.

The next step to the development of the sensor would be to incorporate basic silhouette

detection algorithms so that the system can be used as an early warning detector against animal intrusion. The sensor also needs to be deployed in the field to test weatherproofing and power consumption.

7 Conclusions

The report presented the design, development and evaluation of a high resolution silhouette detection and ranging sensor. The sensor was evaluated and was found to be accurate with < 1 inch resolution in height. Wireless communication, local datalogging, solar charging and weatherproofing were incorporated into the sensor. As a consequence, the sensor is well suited for monitoring intrusions in field conditions. In particular, the high resolution in measuring height enables the sensor to be used for collecting demography information on wild elephants.

8 Acknowledgments

We acknowledge financial support from DBT-IISc partnership program(to Dr. Vishwesh Guttal).

The author would like to thank Dr. Karpagam Chelliah for helpful discussions and continued moral support.

References

- [1] Mahapatra, E.; Sathishkumar, P.; Jayanth, G.R., "An Opto-Electronic Profiling and Ranging Sensor for Monitoring of Perimeters," Sensors Journal, IEEE , vol.PP, no.99, pp.1,1
- [2] Chelliya Arivazhagan and Raman Sukumar "Constructing Age Structures of Asian Elephant Populations: A Comparison of Two Field Methods of Age Estimation" Gajah 29 (2008) 11-16
- [3] F. Della Rocca, "How tall is an elephant? Two methods for estimating elephant height" Web Ecol., 7, 1-10, 2007
- [4] S. Wijeyamohan et. al. "A simple technique to estimate linear body measurements of elephants " Scientific Correspondence Current Science, vol. 102, no. 1, 10 January 2012
- [5] Russomanno, David; Chari, Srikant; Halford, Carl "Sparse Detector Imaging Sensor with Two-Class Silhouette Classification" Sensors Journal, IEEE , vol. 10, no. 6, June 2010
- [6] Sukumar, R., Joshi, N.V. and Krishnamurthy, V. (1988). "Growth in the Asian elephant." Proceedings of the Indian Academy of Sciences (Animal Sciences)97: 561-571